Hadron formation in high energy photonuclear reactions

T. Falter and U. Mosel

Institut fuer Theoretische Physik, Universitaet Giessen, D-35392 Giessen, Germany

We present a new method to account for coherence length effects in a semiclassical transport model. This allows us to describe photoproduction and electroproduction at large nuclei ($A > 12$) and high energies using a realistic coupled channel description of the final state interactions that goes beyond simple Glauber theory. We show that the purely absorptive treatment of the final state interactions can lead to wrong estimates of color transparency and formation time effects in particle production. As an example, we discuss exclusive ρ^0 photoproduction on Pb at a photon energy of 7 GeV as well as K^+ production in the photon energy range 1–7 GeV.

I. INTRODUCTION

In a high energy collision between two hadrons or a photon and a hadron it takes a finite amount of time for the reaction products to evolve to physical particles. During the collision process some momentum transfer between the hadrons or some hard scattering between two of the hadrons' constituents leads to the excitation of hadronic strings. The time that is needed for the creation and fission of these strings as well as for the hadronization of the string fragments cannot be calculated within perturbative QCD because the hadronization process involves small momentum transfers of typically only a few hundred MeV. One can perform an estimate of the formation time τ_f in the rest frame of the hadron. It should be of the order of the time that the quark-antiquark (quark-diquark) pair needs to reach a separation, which is of the size of the produced hadron ($r_h \approx 0.6$–0.8 fm):

$$\tau_f \gtrsim \frac{r_h}{c}. \qquad (1.1)$$

During their evolution to physical hadrons the reaction products will react with reduced cross sections. This is motivated by means of color transparency: the strings and the substrings created during the fragmentation are in a color singlet state and therefore react with a cross section that increases with their transverse size. As a consequence the produced hadrons travel inside the nuclear medium with a reduced scattering probability during their formation time. Hence the formation time plays an important role in the dynamics of nuclear reactions, e.g., heavy-ion collisions and proton- and pion-induced reactions as well as photon- and electron-induced reactions on nuclei.

The latter two are of special interest because they are less complex than heavy-ion collisions and, in contrast to hadron-induced reactions, the primary reaction in general does not only take place at the surface of the nucleus but also at larger densities. Experiments at TJNAF and DESY, for example, deal with exclusive and semi-inclusive meson photoproduction and electroproduction at high energies. Large photon energies E_γ are of special interest because of time dilatation the formation length l_f in the rest frame of the nucleus can exceed nuclear dimensions:

$$l_f = v_h \gamma \tau_f = \frac{p_h}{m_h} \tau_f. \qquad (1.2)$$

If one chooses the formation time to be $\tau_f = 0.8$ fm/c, the formation length in the rest frame of the nucleus will be about 30 fm for a 5 GeV pion and about 7 fm for a 5 GeV kaon or a 7 GeV ρ meson. These lengths have to be compared with the typical size of nuclear radii, e.g., 2.7 fm for ^{12}C and 7.1 fm for ^{208}Pb. Because it suppresses the final state interactions, the formation time has a big effect on photonuclear production cross sections at high energies. Turning this argument around, exclusive and semi-inclusive photoproduction of mesons on nuclei [1] offer a possibility to study these formation times if the FSI are well under control.

Usually, the FSI are modeled within Glauber theory [2,3] and treated as purely absorptive. A more realistic description of the FSI has to take also regeneration of the mesons studied into account. For this we use a coupled channel semiclassical transport model based on the Boltzmann-Uehling-Uhlenbeck (BUU) equation. Originally developed to describe heavy-ion collisions [4] at SIS energies it has been extended in later works to investigate also inclusive particle production in heavy-ion collisions up to $200A$ GeV and π- [5] and p induced as well as photon- and electron-induced reactions in the resonance region [6]. Inclusive photoproduction of mesons at energies between 1 and 7 GeV has been investigated in Ref. [7]. An attractive feature of this model is its capability to describe a large variety of very different reaction types in a consistent way.

Since photon-induced reactions are known to be shadowed ($\sigma_{\gamma A} < A \sigma_{\gamma N}$) above photon energies of approximately 1 GeV [8–10], one needs a way to account for this shadowing effect in photoproduction. This is straightforward within Glauber theory, but it is not clear how to account for this initial state coherence length effect in a semiclassical transport model for the FSI. A first attempt at combining the quantum mechanical coherence in the entrance channel with our incoherent treatment of the FSI has been made in Ref. [7]. In Sec. II we present a new, improved way to implement

shadowing in our model. In Sec. III the results for exclusive ρ^0 photoproduction on ^{208}Pb at 7 GeV are compared with the predictions from simple Glauber theory. In Sec. III we also demonstrate the importance of the coupled channel treatment of the FSI by looking at the nuclear K^+ photoproduction cross section. We summarize our results in Sec. IV.

II. MODEL

In this section we describe how we account for shadowing in our model and only sketch the principles of the transport model itself. For a detailed description of the transport model used we refer to Ref. [11]. In our model the incoherent reaction of a high energy photon with a nucleus takes place in two steps. In the first step the photon reacts with one nucleon inside the nucleus (impulse approximation) and produces some final state X. In this process nuclear effects such as Fermi motion, binding energies, and Pauli blocking of the final state nucleons are taken into account. In the second step the final state X is propagated within the transport model. Except for the elastic vector meson and exclusive strangeness production (see Ref. [7]) we use the Lund string model FRITIOF [12] to describe high energy photoproduction on the nucleon. The same string model is also used to deal with high energy particle collisions in the FSI. Since FRITIOF does not accept photons as incoming particles, ρ dominance was used in Ref. [7] and the photon was passed as a massless ρ^0. This led to an excellent description of charged particle multiplicities in γp collisions.

Here we generalize to vector meson dominance (VMD) [13] by writing the incoming photon state as

$$|\gamma\rangle = \left(1 - \sum_{V=\rho,\omega,\phi} \frac{e^2}{2g_V^2}\right)|\gamma_0\rangle + \sum_{V=\rho,\omega,\phi} \frac{e}{g_V}|V\rangle, \quad (2.1)$$

and pass the photon as a massless ρ^0, ω, or ϕ with a probability corresponding to the strength of the vector meson coupling to the photon times its nucleonic cross section σ_{VN},

$$P(V) = \frac{(e/g_V)^2 \sigma_{VN}}{\sigma_{\gamma N}}. \quad (2.2)$$

These probabilities follow from using Eq. (2.1) in the optical theorem:

$$\sigma_{\gamma N} = \left(1 - \sum_{V=\rho,\omega,\phi} \frac{e^2}{2g_V^2}\right)^2 \sigma_{\gamma_0 N} + \sum_{V=\rho,\omega,\phi} \left(\frac{e}{g_V}\right)^2 \sigma_{VN}. \quad (2.3)$$

As can be seen from Eqs. (2.1) and (2.3) there is also a finite probability

$$P(\gamma_0) = 1 - \sum_{V=\rho,\omega,\phi} P(V) \quad (2.4)$$

that the "bare" photon γ_0 has to be passed to FRITIOF; the component γ_0 does not get shadowed in the nucleus. In a generalized VMD model, for example, the γ_0 includes contributions from heavy intermediate hadronic states, which, as
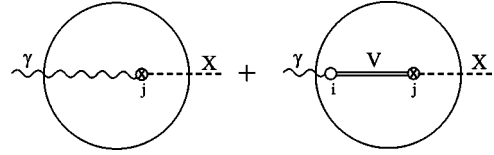

FIG. 1. The two amplitudes of order α_{em} that contribute to incoherent meson photoproduction in simple Glauber theory. The left amplitude alone would lead to an unshadowed cross section. Its interference with the right amplitude gives rise to shadowing.

we show later, are not shadowed because of the large momentum transfer q_V that is needed to put them on their mass shell. Since FRITIOF does not accept a "bare" photon as input we replace it again by a vector meson $V(=\rho^0, \omega$ or $\phi)$, with the probability

$$P_{\gamma_0}(V) = \frac{(e/g_V)^2 \sigma_{VN}}{\displaystyle\sum_{V'=\rho,\omega,\phi} (e/g_{V'})^2 \sigma_{V'N}}. \quad (2.5)$$

The particle production in FRITIOF can be decomposed into two parts. First there is a momentum transfer taking place between the two incoming hadrons, leaving two excited strings with the quantum numbers of the initial hadrons. After that the two strings fragment into the observed particles. As a formation time we use 0.8 fm/c in the rest frame of each hadron; during this time the hadrons do not interact with the rest of the system.

Up to now we did not take shadowing into account. In Glauber theory this corresponds to using only the left amplitude in Fig. 1, where a photon directly produces some hadron X at nucleon j. The left amplitude alone leads to the unshadowed incoherent photoproduction cross section

$$\sigma_{\gamma A \to XA*}^{\text{unshadowed}} = \sigma_{\gamma N \to XN} \int d^2b \int dz_j \tilde{n}(\vec{b}, z_j)$$

$$\times \exp\left(-\sigma_{XN} \int_{z_j}^{\infty} dz\, n(\vec{b}, z)\right), \quad (2.6)$$

where $n(\vec{r})$ denotes the nucleon number density, $\tilde{n}(\vec{r})$ the number density of nucleons with the correct charge to produce the hadron X, and σ_{XN} is the total XN cross section. The exponential damping factor in Eq. (2.6) describes the absorption of the particle X on its way out of the nucleus.

In Glauber theory shadowing arises from the interference of the left amplitude in Fig. 1 with the second amplitude of order α_{em}, which is shown on the right-hand side. In this process the photon produces a vector meson V on nucleon i without excitation of the nucleus. This vector meson then scatters at fixed impact parameter $\vec{b}$ (eikonal approximation) through the nucleus to nucleon j and produces the final state meson X, leaving the nucleus in the same excited state as in the direct process. Off-diagonal scattering, where a vector meson V scatters into a different vector meson V', is usually neglected. In view of the upcoming discussion of exclusive ρ^0 photoproduction on Pb we state here the Glauber result [3] for the incoherent vector meson production cross section:

$$\sigma_{\gamma A \to VA*} = \sigma_{\gamma N \to VN} \int d^2b \int_{-\infty}^{\infty} dz_j n(\vec{b}, z_j)$$

$$\times \exp\left(-\sigma_{VN} \int_{z_j}^{\infty} dz\, n(\vec{b}, z)\right)$$

$$\times \left| 1 - \int_{-\infty}^{z_j} dz_i n(\vec{b}, z_i) \frac{\sigma_{VN}}{2} (1 - i\alpha_V) e^{iq_V z_i} \right.$$

$$\left. \times \exp\left[-\frac{1}{2}\sigma_{VN}(1 - i\alpha_V)\int_{z_i}^{z_j} dz\, n(\vec{b}, z)\right] \right|^2. \tag{2.7}$$

Again $n(\vec{r})$ denotes the nucleon number density, σ_{VN} the total VN cross section, and α_V the ratio of the real to imaginary part of the VN forward scattering amplitude. The momentum transfer

$$q_V \approx m_V^2 / 2E_\gamma \tag{2.8}$$

arises from putting the vector meson on its mass shell. A large momentum transfer q_V is suppressed by the elastic nuclear form factor and leads to less shadowing due to the oscillating factor $\exp[iq_V z_i]$ in the integrand of Eq. (2.7). Note that q_V is just the inverse of the coherence length, i.e., the distance, given by the uncertainty principle, which the photon can travel as a V fluctuation. For the quantities in Eq. (2.7) we use the parametrizations of Model I of Ref. [13] with which one obtains a very good description of the shadowing effect in nuclear photoabsorption down to the onset region [9,10].

One clearly sees from Eq. (2.7) how the FSI separate from the "initial state interactions" of the photon. We now replace the exponential damping factor $\exp[-\sigma_{VN}\int_{z_j}^{\infty} dz\, n(\vec{b},z)]$, which corresponds to purely absorptive FSI, by a transport model. This allows us to incorporate a wider class of FSI. In addition we want to include events where the final vector meson V is not produced in the primary reaction but via sidefeeding. This leads to less reduction of the nuclear production cross section even with the same σ_{VN}. We thus also need to know how all the other possible primary reactions are shadowed. We, therefore, start from Eq. (2.1) and use Glauber theory to calculate how the single V components of the photon change due to multiple scattering on the way to nucleon j where the state X is produced [3]:

$$|\gamma(\vec{r}_j)\rangle = \left(1 - \sum_{V=\rho,\omega,\phi} \frac{e^2}{2g_V^2}\right) |\gamma_0\rangle$$

$$+ \sum_{V=\rho,\omega,\phi} \frac{e}{g_V} [1 - \overline{\Gamma_V}(\vec{r}_j)] |V\rangle. \tag{2.9}$$

Here the (photon-energy-dependent) nuclear profile functions for the different vector meson components V are given as
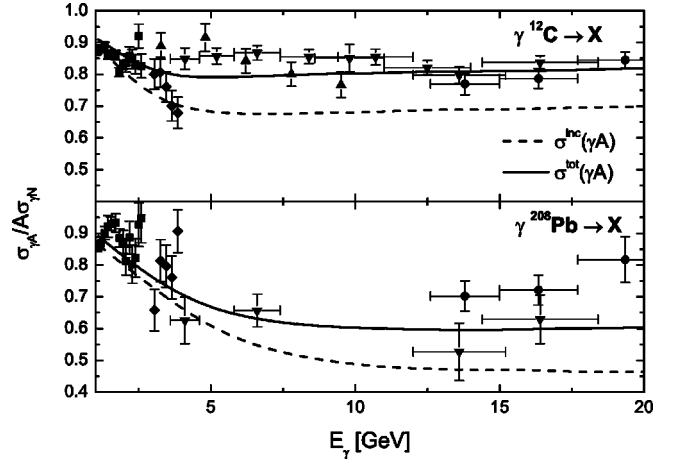

FIG. 2. The nuclear photoabsorption cross section divided by $A\sigma_{\gamma N}$ plotted versus the photon energy E_γ. The solid line represents the result of Ref. [9] for the total photon nucleus cross section. The dashed line shows the contribution from incoherent reactions to $\sigma_{\gamma A}^{tot}$ and is calculated using Eq. (2.12). More than 90% of the difference between $\sigma_{\gamma A}^{inc}$ and $\sigma_{\gamma A}^{tot}$ is due to coherent ρ^0 photoproduction.

$$\overline{\Gamma_V}(\vec{b}, z_j) = \int_{-\infty}^{z_j} dz_i n(\vec{b}, z_i) \frac{\sigma_{VN}}{2}(1 - i\alpha_V) e^{iq_V(z_i - z_j)}$$

$$\times \exp\left[-\frac{1}{2}\sigma_{VN}(1 - i\alpha_V)\int_{z_i}^{z_j} dz\, n(\vec{b}, z)\right]. \tag{2.10}$$

Note that the γ_0 component is, by definition, not modified due to the presence of the nuclear medium. The cross section for the photon to react with nucleon j at position $\vec{r}_j$ inside the nucleus can be deduced via Eq. (2.9) from the optical theorem:

$$\sigma_{\gamma N}(\vec{r}_j) = \left(1 - \sum_{V=\rho,\omega,\phi} \frac{e^2}{2g_V^2}\right)^2 \sigma_{\gamma_0 N}$$

$$+ \sum_{V=\rho,\omega,\phi} \left(\frac{e}{g_V}\right)^2 |1 - \overline{\Gamma_V}(\vec{r}_j)|^2 \sigma_{VN}. \tag{2.11}$$

As for the photon in vacuum each term gives the relative weight for the corresponding photon component to be passed to FRITIOF. When integrated over the whole nucleus one gets from Eq. (2.11) the total incoherent photonuclear cross section

$$\sigma_{\gamma A}^{inc} = \int d^3r_j n(\vec{r}_j) \sigma_{\gamma N}(\vec{r}_j), \tag{2.12}$$

which is shown in Fig. 2 by the dashed line together with the total nuclear photoabsorption cross section as derived from the optical theorem in Ref. [9]:
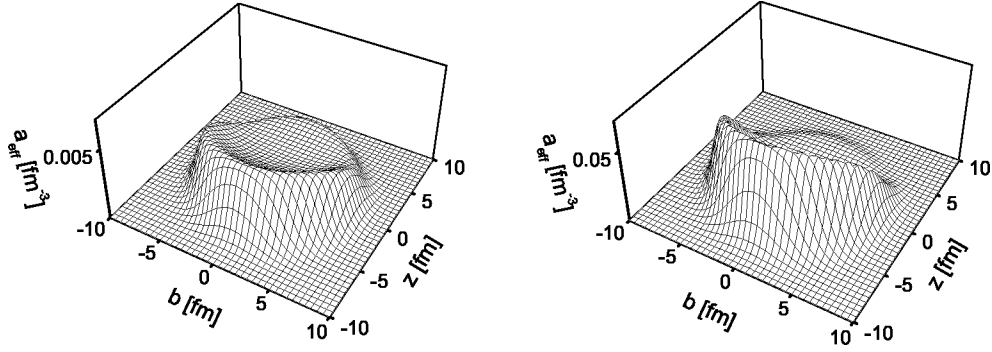
FIG. 3. The number density of nucleons that react with the ϕ component (left side) and ρ^0 component (right side) of a 20 GeV photon for ^{208}Pb calculated using Eq. (2.14). In both cases the nucleons on the front side of the nucleus shadow the downstream nucleons. This effect is stronger for the ρ^0 component because of its larger nucleonic cross section.

$$\sigma_{\gamma A}^{tot} = A\,\sigma_{\gamma N} - \sum_{V=\rho,\omega,\phi} \frac{k_V}{2k}\left(\frac{e}{g_V}\right)^2 \mathrm{Re}\left\{\sigma_{VN}^2(1-\alpha_V)^2\int d^2b\right.$$

$$\times \int_{-\infty}^{\infty} dz_i \int_{z_i}^{\infty} dz_j\, n(\vec{b},z_i)n(\vec{b},z_j)e^{iq_V(z_i-z_j)}$$

$$\left.\times \exp\left[-\frac{1}{2}\sigma_{VN}(1-i\alpha_V)\int_{z_i}^{z_j}dz'\,n(\vec{b},z')\right]\right\}. \quad (2.13)$$

Here k and k_V denote the momentum of the photon and the vector meson, respectively, and we again use the parametrizations of Model I of Ref. [13]. More than 90% of the difference between those two cross sections stems from coherent ρ^0 photoproduction.

In Fig. 3 we show how strongly the ρ^0 and the ϕ components of a real 20 GeV photon are separately shadowed in Pb. We plot the number density of the nucleons reacting with the V components of the photon

$$a_{eff}^V(\vec{r}_j) = n(\vec{r}_j)\frac{1}{\sigma_{\gamma N}}\left(\frac{e}{g_V}\right)^2 |1-\overline{\Gamma_V(\vec{r}_j)}|^2 \sigma_{VN} \quad (2.14)$$

as a function of $\vec{r}_j$. One clearly sees that due to its smaller nucleonic cross section the ϕ component is less shadowed than the ρ^0 component at the backside of the nucleus. As a consequence strangeness production (e.g., K photoproduction), where the primary reaction is preferably triggered by the ϕ component of the photon, is less shadowed than, e.g., π photoproduction. This dependence of the strength of shadowing on the reaction type is new compared to the treatment of shadowing in Ref. [7] and can also be seen directly from the second amplitude in Fig. 1 because of the occurrence of the scattering process $VN\rightarrow XN$ at nucleon j.

As already mentioned above the purely absorptive FSI of the Glauber model are very different from the coupled channel description of a transport model. The transport model we use is based on the BUU equation that describes the time evolution of the phase space density $f_i(\vec{r},\vec{p},t)$ of particles of type i that can interact via binary reactions [11]. In our case these particles are the nucleons of the target nucleus as well as the baryonic resonances and mesons ($\pi,\eta,\rho,K,\dots$) that

can either be produced in the primary γN reaction or during the FSI. For particles of type i the BUU equation looks as follows:

$$\left(\frac{\partial}{\partial t} + \frac{\partial H}{\partial \vec{r}}\frac{\partial}{\partial \vec{r}} - \frac{\partial H}{\partial \vec{r}}\frac{\partial}{\partial \vec{p}}\right)f_i(\vec{r},\vec{p},t)$$

$$= I_{coll}[f_1,\dots,f_i,\dots,f_M]. \quad (2.15)$$

In the case of baryons the Hamilton function H includes a mean field potential, which in our model depends on the particle position and momentum. The collision integral on the right-hand side accounts for the creation and annihilation of particles of type i in a collision as well as elastic scattering from one position in phase space into another. For fermions Pauli blocking is taken into account in I_{coll} via blocking factors. For each particle type i such a BUU equation exists; all are coupled via the mean field and the collision integral. This leads to a system of coupled differential-integral equations that we solve via a test particle ansatz for the phase space density (for details see Ref. [11]). Since the collision integral also accounts for particle creation in a collision the observed outgoing particle X cannot only be produced in the primary reaction, but can also be created by sidefeeding in which a particle Y is created first, which propagates, and then, by FSI, produces X. In addition the state X might get absorbed on its way out of the nucleus but be fed in again in a later interaction. Both cases can *a priori* not be ignored, but are usually neglected in Glauber models.

III. RESULTS

Exclusive vector meson photoproduction and electroproduction on nuclei are an ideal tool to study effects of the coherence length, formation time and color transparency. Exclusive ρ^0 electroproduction has been investigated in the HERMES experiment [14] at photon energies between 10 GeV and 20 GeV and virtuality $Q^2 \lesssim 5$ GeV^2. The calculations for meson production on nuclei are usually done within the Glauber theory [15]. As already mentioned above the FSI in Glauber theory are usually purely absorptive. This means that for the reaction $\gamma A\rightarrow\rho^0 A^*$ the primary reaction has to be $\gamma N\rightarrow\rho^0 N$. If one treats the FSI via an absorptive
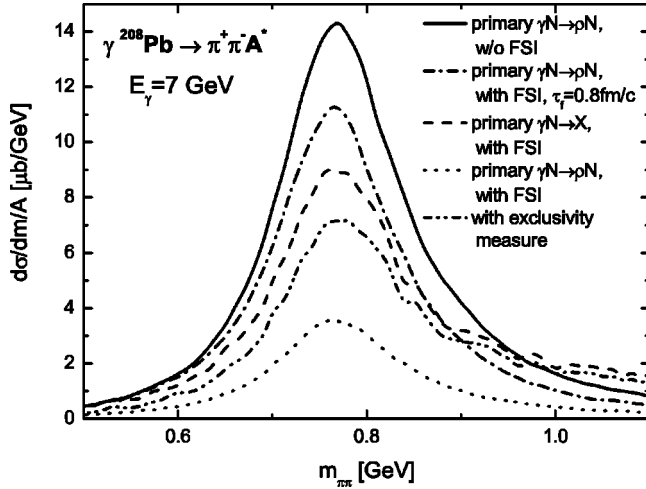
FIG. 4. Mass differential cross section for exclusive ρ^0 production on ^{208}Pb at $E_\gamma = 7$ GeV. The meaning of the different curves is explained in detail in the text. All the curves, except the one with the explicitly given formation time $\tau_f = 0.8$ fm/c, have been calculated with $\tau_f = 0$. The fluctuations in the dashed and dash-dot-dotted curves are statistical only.

optical potential one gets an exponential damping $\sim \exp[-\sigma_{\rho N} \int_{z_j}^{\infty} dz\, n(\vec{b}, z)]$ of the nuclear production cross section.

We are presently working at incorporating also incoming virtual photons into the formalism developed in Sec. II and at enlarging the configuration space for the FSI. Here we discuss, therefore, only results obtained with real photons and at a lower energy. In Fig. 4 we show the results of our model for the mass differential cross section of incoherent, exclusive ρ^0 photoproduction on ^{208}Pb for $E_\gamma = 7$ GeV. In this case "exclusive" means that the final state consists of a $\pi^+ \pi^-$ pair and 208 bound nucleons. The solid line represents a calculation with the primary reaction restricted to $\gamma N \rightarrow \rho^0 N$. It already includes the effects of shadowing, Fermi motion, Pauli blocking, and the nucleon potential, but no FSI. The dotted line shows the effect of the FSI without a formation time of the ρ^0 in $\gamma N \rightarrow \rho^0 N$. The Glauber model yields quantitatively the same effect of the FSI. This means that in this case (only $\gamma N \rightarrow \rho^0 N$ as primary reaction) FSI processes like $\rho^0 N \rightarrow \pi N$, $\pi N \rightarrow \rho^0 N$, where the primary ρ^0 gets absorbed first and is fed into the outgoing channel by a later FSI, are negligible. If one assumes a formation time of $\tau_f = 0.8$ fm/c for the ρ^0, one gets the result indicated by the dash-dotted line. Due to the finite formation time there is considerably less absorption and the nuclear production cross section increases. If the observed spectrum looked like this, one would in Glauber theory be led to the conclusion of a finite ρ^0 formation time.

However, one will get a similar result with $\tau_f = 0$ if one allows for other primary reaction besides $\gamma N \rightarrow \rho^0 N$ and uses a coupled channel model. This can be seen by looking at the dashed line in Fig. 4. We find that about 60% of the additional ρ^0 stem from inelastic ρ^0 production in the primary reaction, e.g., $\gamma N \rightarrow \rho^0 \pi N$, where the π gets absorbed during the FSI. We now apply an exclusivity measure like the one used in the HERMES experiment [14]
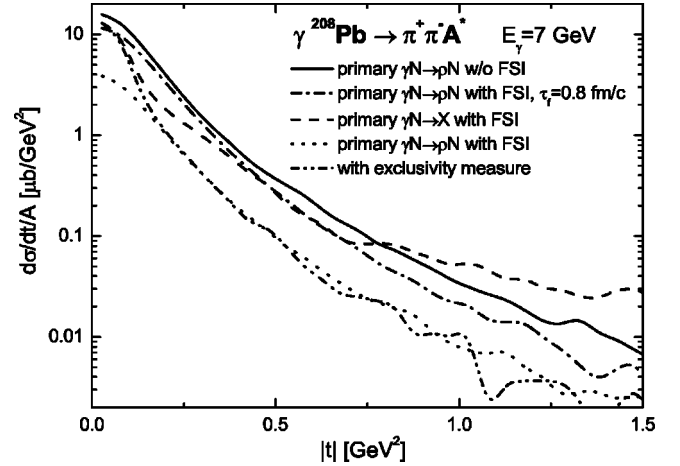

FIG. 5. Calculated $d\sigma/dt$ for exclusive ρ^0 production on ^{208}Pb at $E_\gamma = 7$ GeV. The meaning of the different curves is the same as in Fig. 4. The structures in the curves at large $|t|$ are statistical only.

$$-2 \text{ GeV} < \Delta E = \frac{p_Y^2 - m_N^2}{2 m_N} < 0.6 \text{ GeV}, \qquad (3.1)$$

where m_N is the nucleon mass and

$$p_Y = p_N + p_\gamma - p_\rho \qquad (3.2)$$

is the four-momentum of the undetected final state. Here p_γ and p_ρ denote the four-momenta of the incoming photon and the detected $\pi^+ \pi^-$ pair and p_N is the four-momentum of the struck nucleon, which, for the calculation of p_Y, is assumed to be at rest. Using Eq. (3.1) leads to a decrease of the cross section (dash-dot-dotted line) because some of the inelastic primary events are excluded. If the exclusivity measure was good enough to single out only the elastic $\gamma N \rightarrow \rho^0 N$ reactions from the primary events, the dash-dot-dotted curve would coincide with the dotted line and Glauber theory would be applicable. Since this is not the case, one still extracts a too large formation time when using Glauber theory.

One therefore needs a further constraint in addition to the exclusivity measure (3.1), which becomes apparent by looking at the differential cross section $d\sigma/dt$ in Fig. 5; the meaning of the lines is as before. For $|t| > 0.1$ GeV^2 the full calculation with exclusivity measure (dash-dot-dotted line) gives the same result as the one with the primary reaction $\gamma N \rightarrow \rho^0 N$ and FSI (dotted line). In this kinematic regime Glauber theory can therefore be used. For $|t| < 0.1$ GeV^2, however, the exclusivity measure (3.1) cannot distinguish between elastic ρ^0 photoproduction ($\gamma N \rightarrow \rho^0 N$) and other primary reactions, e.g., inelastic ρ^0 photoproduction ($\gamma N \rightarrow \rho^0 X$, $X \neq N$). At low values of $|t|$ there exist many states X with invariant masses that are not excluded by the exclusivity measure (3.1). In addition we find that about 25% of the finally accepted ρ^0 in this t region are not produced in the primary reaction but stem from sidefeeding in the FSI. In the HERMES experiment one makes a lower $|t|$ cut to get rid of the coherent ρ^0 photoproduction contribution. In the case of lead and $E_\gamma = 7$ GeV the coherent part can be neglected above $|t| \approx 0.05$ GeV^2. For Glauber theory to be reliable one
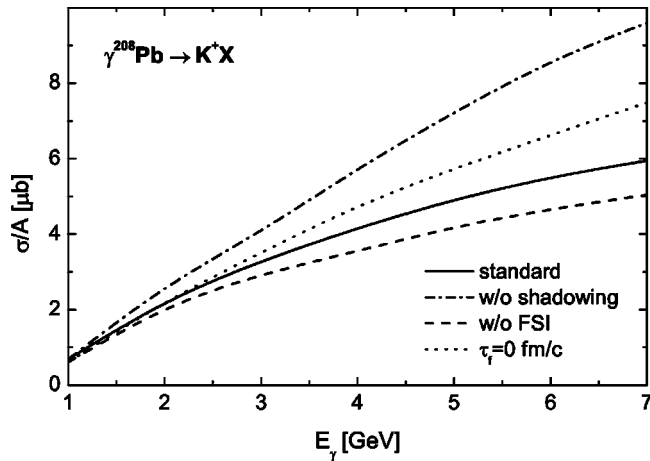
FIG. 6. Photoproduction cross section for K^+ on ^{208}Pb plotted as a function of the photon energy. The solid line represents the full calculation. The dash-dotted line shows the result without shadowing of the incoming photon, the dashed line the result without FSI, and the dotted line the calculation without formation time.

has to increase this threshold to approximately $|t| = 0.1$ GeV^2. Glauber theory can thus be trusted only under certain kinematic constraints.

So far we have discussed a case in which a strongly interacting particle, the ρ^0 meson, is produced. In the following we will now discuss the special effects that appear in a coupled channel treatment of the FSI when a weakly interacting particle, such as the K^+ meson, is considered. In Fig. 6 we therefore show the cross section for the reaction $\gamma A \rightarrow K^+ X$ in the photon energy range 1–7 GeV for ^{208}Pb. This reaction had already been investigated in Ref. [7]; the new treatment of shadowing and the initial interactions as outlined in Eqs. (2.1)–(2.5) lead to an increase of the total yield at 7 GeV by about 20%. The solid curve in Fig. 6 represents the results of the full calculation (including shadowing, FSI, $\tau_f = 0.8$ fm/c, etc.). By comparison with the calculation without shadowing (dash-dotted line) one sees how impor-

tant shadowing becomes with increasing photon energy. At 7 GeV it reduces the nuclear production cross section to about 65%.

The importance of a coupled channel treatment of the FSI becomes clear when comparing the full calculation with the one without FSI (dashed line). Since the $\bar{s}$ quark cannot be absorbed in medium the FSI can just increase the K^+ yield via processes like $\pi N \rightarrow K^+ Y$ ($Y = \Sigma, \Lambda$), for example. With decreasing formation time the primarily produced pions have a greater chance to produce K^+ in the FSI. As a consequence of this, a shorter formation time will lead to an increase of the nuclear K^+ photoproduction cross section as can be seen from the dotted line. An enhancement of the K^+ production cross section due to FSI cannot be explained by purely absorptive FSI as in simple Glauber theory, where it would necessarily be interpreted as being due to a longer formation time of the K^+.

IV. SUMMARY

High energy photoproduction off nuclei offers a promising possibility to study the physics of hadron formation. Necessary for such studies is a reliable model of the FSI to extract the formation time from the production cross sections. Whereas Glauber models allow for a straightforward implementation of the nuclear shadowing effect they usually have the disadvantage of a purely absorptive treatment of the FSI. As we have shown the latter can lead to a wrong estimate of the formation time. A more realistic treatment of the FSI is possible within a coupled channel transport model. We have presented a method to combine such an incoherent treatment of FSI with coherence length effects in the entrance channel which can easily be extended to higher energies and virtual photons. We have shown that in particular the production of mesons with long mean free path will be affected by the coupled channel effects in the FSI.

[1] A. Airapetian *et al.*, Eur. Phys. J. C **20**, 479 (2001).

[2] R.J. Glauber, in *Lectures in Theoretical Physics*, edited by W.E. Brittin and L.G. Dunham (Wiley Interscience, New York, 1959), Vol. I, p. 315; R.J. Glauber, in *High Energy Physics and Nuclear Structure*, edited by S. Devons (Plenum, New York, 1970), p. 207.

[3] D.R. Yennie, in *Hadronic Interactions of Electrons and Photons*, edited by J. Cummings and H. Osborn (Academic, New York, 1971), p. 321.

[4] G. Wolf, W. Cassing, and U. Mosel, Nucl. Phys. **A552**, 549 (1993); S. Teis, W. Cassing, M. Effenberger, A. Hombach, U. Mosel, and G. Wolf, Z. Phys. A **356**, 421 (1997); A. Hombach, W. Cassing, S. Teis, and U. Mosel, Eur. Phys. J. A **5**, 157 (1999).

[5] M. Effenberger, E.L. Bratkovskaya, W. Cassing, and U. Mosel, Phys. Rev. C **60**, 027601 (1999).

[6] M. Effenberger, A. Hombach, S. Teis, and U. Mosel, Nucl.

Phys. **A614**, 501 (1997); J. Lehr, M. Effenberger, and U. Mosel, *ibid.* **A671**, 503 (2000).

[7] M. Effenberger and U. Mosel, Phys. Rev. C **62**, 014605 (2000).

[8] N. Bianchi *et al.*, Phys. Rev. C **54**, 1688 (1996); V. Muccifora *et al.*, *ibid.* **60**, 064616 (1999).

[9] T. Falter, S. Leupold, and U. Mosel, Phys. Rev. C **62**, 031602(R) (2000).

[10] T. Falter, S. Leupold, and U. Mosel, Phys. Rev. C **64**, 024608 (2001).

[11] M. Effenberger, E.L. Bratkovskaya, and U. Mosel, Phys. Rev. C **60**, 044614 (1999).

[12] B. Anderson, G. Gustafson, and Hong Pi, Z. Phys. C **57**, 485 (1993).

[13] T.H. Bauer, F. Pipkin, R. Spital, and D.R. Yennie, Rev. Mod. Phys. **50**, 261 (1978).

[14] K. Ackerstaff *et al.*, Phys. Rev. Lett. **82**, 3025 (1999).

[15] J. Hüfner, B. Kopeliovich, and J. Nemchik, Phys. Lett. B **383**, 362 (1996); J. Hüfner and B. Kopeliovich, *ibid.* **403**, 128 (1997); R. Engel, J. Ranft, and S. Roesler, Phys. Rev. D **55**, 6957 (1997); G. Kerley and G. Shaw, *ibid.* **56**, 7291 (1997); A. Pautz and G. Shaw, Phys. Rev. C **57**, 2648 (1998); T. Renk, G. Piller, and W. Weise, Nucl. Phys. **A689**, 869 (2001); B. Kopeliovich, J. Nemchik, A. Schäfer, and A.V. Tarasov, Phys. Rev. C **65**, 035201 (2002).